Mechanism for resistive switching in an oxide-based electrochemical metallization memory

Shanshan Peng, Fei Zhuge, Xinxin Chen, Xiaojian Zhu, Benlin Hu, Liang Pan, Bin Chen, and Run-Wei Li

---

Articles you may be interested in

Effect of ultraviolet illumination on metal oxide resistive memory
Appl. Phys. Lett. **105**, 253111 (2014); 10.1063/1.4904396

Effects of the oxygen vacancy concentration in InGaZnO-based resistance random access memory
Appl. Phys. Lett. **101**, 243503 (2012); 10.1063/1.4770073

Unipolar resistive switching behavior of Pt/Li x Zn1− x O/Pt resistive random access memory devices controlled by various defect types
Appl. Phys. Lett. **101**, 203501 (2012); 10.1063/1.4766725

Switching mechanism transition induced by annealing treatment in nonvolatile Cu/ZnO/Cu/ZnO/Pt resistive memory: From carrier trapping/detrapping to electrochemical metallization
J. Appl. Phys. **106**, 123705 (2009); 10.1063/1.3273329

Endurance enhancement of Cu-oxide based resistive switching memory with Al top electrode
Appl. Phys. Lett. **94**, 213502 (2009); 10.1063/1.3142392

Mechanism for resistive switching in an oxide-based electrochemical metallization memory

Shanshan Peng, Fei Zhuge,[a] Xinxin Chen, Xiaojian Zhu, Benlin Hu, Liang Pan, Bin Chen, and Run-Wei Li[a]

Key Lab of Magnetic Materials and Devices, Ningbo Institute of Material Technology and Engineering, Chinese Academy of Sciences, Ningbo 315201, China and Zhejiang Province Key Lab of Magnetic Materials and Application Technology, Ningbo Institute of Material Technology and Engineering, Chinese Academy of Sciences, Ningbo 315201, China

A comparison of the asymmetric OFF-state current-voltage characteristics between Cu/ZnO/Pt and Cu/ZnO/Al-doped ZnO (AZO) electrochemical metallization memory (ECM) cells demonstrates that the Cu filament rupture and rejuvenation occur at the ZnO/Pt (or AZO) interface, i.e., the cathodic interface. Therefore, the filament is most likely to have a conical shape, with wider and narrower diameters formed at the anodic and cathodic interfaces, respectively. It is inferred that the filament growth starts at the anode surface and stops at the cathode surface. Our results indicate that oxide-based ECM cells strongly differ from sulfide- and selenide-based ones in the resistive switching mechanism. © *2012 American Institute of Physics*. [doi:10.1063/1.3683523]

As a denser, faster and less energy-consuming non-volatile memory, which is based on resistive switching (RS) effects, resistance random access memory (RRAM) has attracted increasing attention.[1] Especially, electrochemical metallization memory (ECM) cells, typically based on the migration of Ag or Cu ions, are promising, due to their maturity with respect to industrialization and the proven scalability potential.[2] The ECM cell consists of an electrode made from an electrochemically active electrode (AE) metal, such as Ag or Cu, an electrochemically inert counter electrode (CE), such as Pt, Ir, W, or Au, and a thin film of a solid electrolyte sandwiched between both electrodes.[3] Besides the "classical" binary sulfides[4–6] and selenides[7–10] and the ternary glassy sulfides[11–13] as a solid electrolyte, various oxides such as ZnO,[14–17] WO_3,[18] SiO_2,[19,20] Ta_2O_5,[21] TiO_2,[22] ZrO_2,[23] and Al_2O_3,[24] amorphous Si (Ref. 25) and C (Ref. 26) have been also employed.

For the RS mechanism of ECM cells, the most widely accepted hypotheses is as follows,[2,3] using Cu as the AE (anode) and Pt as the CE (cathode) metal: (i) anodic dissolution of Cu according to the reaction $Cu \rightarrow Cu^{Z+} + Ze^-$, where Cu^{Z+} represents the Cu^+ or Cu^{2+}; (ii) drift of the Cu^{Z+} cations across the solid-electrolyte film under the high electric field; (iii) reduction and electro-crystallization of Cu on the CE surface according to the reaction $Cu^{Z+} + Ze^- \rightarrow Cu$. The electro-crystallization process leads to the formation of a metal filament. After the filament has grown sufficiently far to make a contact to the opposite Cu electrode, the cell has switched to the ON-state. (iv) A sufficient voltage of opposite polarity is applied and the electrochemical dissolution of the metal filament switches the cell to its initial OFF-state. Steps (i)–(iii) represent the overall "Electroforming" or "SET" process, whereas step (iv) indicates the "RESET" process. Based on the above hypotheses,

one could deduce that (1) the filament growth starts at the CE surface and stops at the AE surface, therefore, the final filament is highly likely to have a conical shape, where wider and narrower diameters are formed at the cathodic and anodic interfaces, respectively; (2) owing to the conical filament shape, it is most likely that the filament rupture and rejuvenation occur at the weakest position along its length, i.e., the anodic interface.[27]

Metal filament formation and rupture are clearly observed in ECM cells based on $Ag/As_2S_3/Au$,[28] Ag/Ag–Ge–Se/Ni,[29] and Cu–GeS/Pt–Ir (Ref. 30) structures, giving direct evidence for the hypotheses described above. Thus, the hypothesis seems tenable in sulfide- and selenide-based ECM cells. Does it apply to oxide-based ECM cells? It is extremely important to clarify this point since the ambiguousness of RS mechanism has severely restricted the development of oxide-based RRAMs. Although there are quite a few references[14,31,32] showing physical evidence of metallic filament formation and rupture in oxide-based cells, several points concerning this filamentary mechanism remain unclear, for example, the exact region where filament rupture and rejuvenation occur.

In our previous study,[15] it has been proven that the RS of Cu/ZnO/Pt sandwiches originates from the formation/rupture of nano-scale Cu filament. In this letter, a comparison of asymmetric current-voltage (*I–V*) characteristics in the OFF-state between Cu/ZnO/Pt and Cu/ZnO/Al-doped ZnO (AZO) ECM cells demonstrates that the metal filament rupture and rejuvenation occur at the cathodic interface, i.e., ZnO/Pt (or AZO) interface. The filament is highly likely to have a conical shape, where wider and narrower diameters are formed at the anodic (Cu) and cathodic (Pt or AZO) interfaces, respectively. It can be inferred from the filament shape that the filament growth starts at the AE (Cu) surface and stops at the CE (Pt or AZO) surface. Therefore, the RS mechanism of oxide-based ECM cells is much different from that of sulfide- and selenide-based ones, likely originating from the

a)Authors to whom correspondence should be addressed. Electronic addresses: zhugefei@nimte.ac.cn and runweili@nimte.ac.cn.

difference of the ion diffusion coefficient between oxides and sulfides and selenides.

Polycrystalline ZnO thin films of thickness 50 nm were deposited on Pt/Ti/SiO$_2$/Si and AZO (resistivity $\sim$10^{-4} Ω cm)/SiO$_2$ substrates at room temperature (RT) by rf magnetron sputtering in Ar/O$_2$ ambient using a ceramic ZnO target.[33–35] Cu top electrodes (AE or anode) of diameter 100 μm were deposited at RT by electron-beam evaporation. The I–V characteristics of the Cu/ZnO/Pt and Cu/ZnO/AZO structures were measured at RT in air using a Keithley 4200 semiconductor parameter analyzer. During the measurement in voltage sweeping mode, the positive bias was defined by the current flowing from the top to the bottom (CE or cathode) electrode, and the negative bias was defined by the opposite direction.

Figures 1(a) and 1(c) illustrate the typical I–V characteristics of the Cu/ZnO/Pt and Cu/ZnO/AZO ECM cells, respectively. Both cells show abrupt SET and RESET processes. Figures 1(b) and 1(d) show the enlarged OFF-state I–V curves of the Cu/ZnO/Pt and Cu/ZnO/AZO cells, respectively. The important feature of Figs. 1(b) and 1(d) is the asymmetry of both I–V curves with respect to the bias voltage. It is interesting that for the Cu/ZnO/Pt cell, the current at a positive bias voltage is lower than that under a negative bias, whereas in the case of the Cu/ZnO/AZO cell, the circumstance is just the reverse. Note that such asymmetries are highly reproducible. In the case of the Cu/ZnO/Pt cell, more than 500 I–V curves have been examined, only 18 curves do not exhibit such an asymmetry as is shown in Fig. 1(b). As for the Cu/ZnO/AZO cell, more than 200 I–V curves have been examined, only 19 curves do not exhibit such an asymmetry as is shown in Fig. 1(d).

In order to understand the intrinsic meaning of different asymmetric I–V characteristics in the OFF-states of Cu/ZnO/Pt and Cu/ZnO/AZO, we first need to discuss the ideal I–V of the various possible OFF-states of the ECM cells. Many speculations are found in the literature concerning the morphology of the metal filament. Often, there are results which

seem to indicate exactly one filament.[2,3,27] Furthermore, in ECM cells, the filament rupture and rejuvenation always occur at a localized position.[2,27] The ideal I–V characteristics of the ON-state and three possible OFF-states (i.e., OFF-1, OFF-2, and OFF-3) of Cu/ZnO/Pt (or AZO) cells are schematically illustrated in Fig. 2. Figure 2(a) shows Ohmic behavior of the ON-state of the ECM cells where the metal filament connects the AE and CE. Compared to the ON-state, I–V characteristics of the OFF-state are more complicated. Figures 2(b)–2(e) illustrate schematic I–V curves of three possible OFF-states of the memory cells where the switching may occur at three different positions, i.e., Cu/ZnO interface (OFF-1), middle part of the ZnO film (OFF-2), and ZnO/Pt (OFF-3 (Pt)) or ZnO/AZO (OFF-3 (AZO)) interface. In the OFF-state, I–V characteristics of the device are dominated by the insulating gap (i.e., ZnO) sandwiched between the electrode and remaining metal filament (OFF-1 and OFF-3, i.e., Cu/gap/Cu and Cu/gap/Pt (or AZO), respectively) or two filament segments (OFF-2, i.e., Cu/gap/Cu). Under the circumstances of OFF-1 and OFF-2, the structures correspond to two back-to-back symmetric Schottky barriers (SBs) at Cu/gap junctions, resulting in symmetric I–V curves with respect to the bias voltage, as schematically shown in Figs. 2(b) and 2(c). However, in the case of OFF-3, the I–V should be asymmetric due to different electrode materials sandwiching the insulating gaps. For the Cu/gap (ZnO)/Pt sandwich, i.e., OFF-3 (Pt), the corresponding band structure is asymmetric due to different SB heights of Cu/ZnO ($\sim$0.45 eV) and Pt/ZnO ($\sim$0.75 eV),[36] as schematically illustrated in the inset of Fig. 2(d). When a bias voltage is applied, one SB is under reverse bias, while the other is forward biased. The impedance will always be dominated by characteristics of the reverse-biased SB.[37] So, at a positive bias, the impedance is dominated by the Pt/ZnO SB; while at a negative bias, the impedance should be dominated by the Cu/ZnO SB. Consequently, the different SB heights result in an asymmetric I–V curve where the current at a negative bias voltage is higher than the positive bias induced one, as
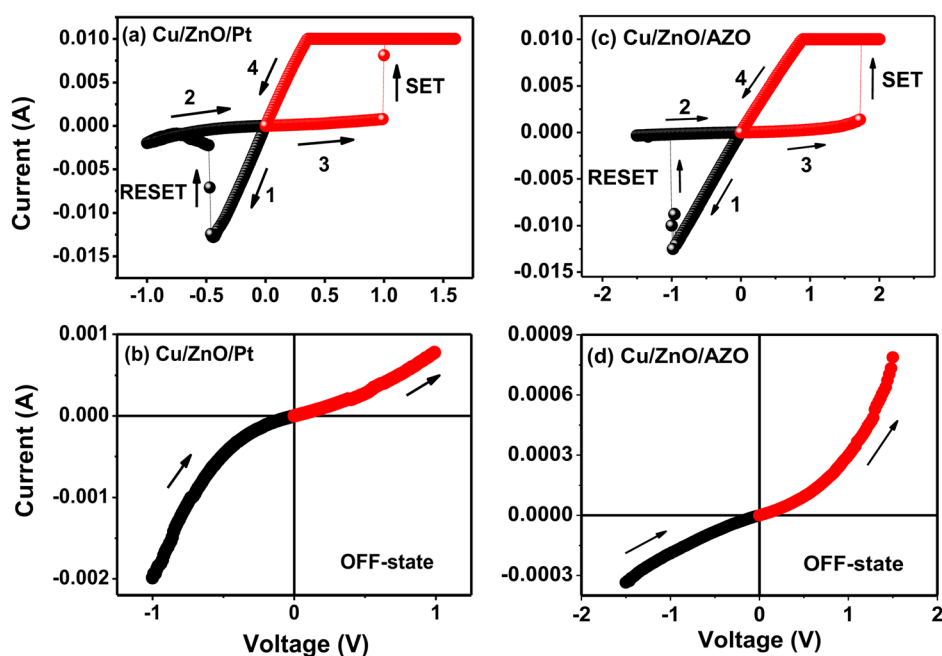
FIG. 1. (Color online) Typical I–V characteristics of the (a) Cu/ZnO/Pt and (c) Cu/ZnO/AZO ECM cells. (b) and (d) Enlarged OFF-state I–V curves of Cu/ZnO/Pt and Cu/ZnO/AZO cells.
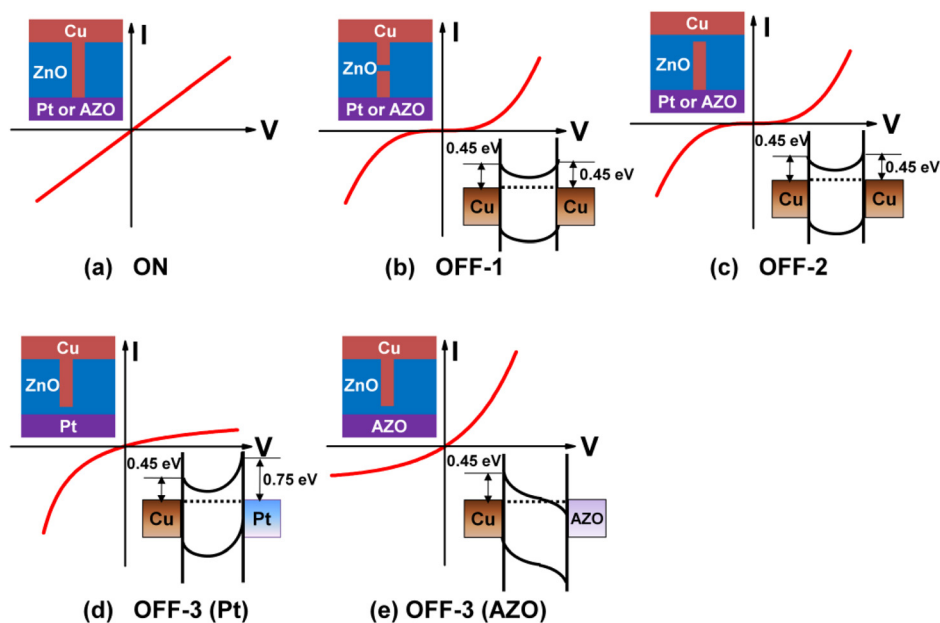
FIG. 2. (Color online) Schematic ideal *I–V* characteristics of the (a) ON-state and (b)–(e) three possible OFF-states (i.e., OFF-1, OFF-2, and OFF-3) of the Cu/ZnO/Pt (or AZO) ECM cells. The insets schematically illustrate the ON-state and three possible OFF-states of the cells and the corresponding band diagrams of the insulating gaps (i.e., ZnO) sandwiched between Cu electrode and Cu filament (OFF-1), Cu filaments (OFF-2), and Cu filament and Pt (OFF-3 (Pt)) or AZO (OFF-3 (AZO)) electrode.

schematically shown in Fig. 2(d). While in the case of the Cu/gap (ZnO)/AZO sandwich, i.e., OFF-3 (AZO), the structure comprises of a Cu/ZnO SB and a ZnO/AZO Ohmic contact junction, as schematically illustrated in the inset of Fig. 2(e), since the work function of metallic AZO (4.26 eV) is lower than that of ZnO (4.45 eV).[38–40] The existence of a single Cu/ZnO SB leads to an asymmetric *I–V* curve where the current at a positive bias voltage is higher than that under a negative bias, as schematically shown in Fig. 2(e).

By comparing *I–V* characteristics shown in Figs. 1 (experimental data) and 2 (schematic diagrams of ideal *I–V* characteristics of three possible OFF-states), one can concluded that OFF-3 is the real OFF-state of Cu/ZnO/Pt (or AZO) ECM cells, i.e., the Cu filament rupture and subsequent rejuvenation occur at the ZnO/Pt (or AZO) interface. The cases of OFF-1 and OFF-2 can be excluded. Considering that the filament is always ruptured at the weakest position along its length,[2,3,27] the Cu filament should have a conical shape, where wider and narrower diameters are formed at the anodic (AE, i.e., Cu) and cathodic (CE, i.e., Pt or AZO) interfaces, respectively, as schematically illustrated in Fig. 3(d). Actually, such conical metal filament shape has been directly observed by transmission electron microscopy in Ag/ZnO/Pt ECM cells.[14] It can be inferred from the conical

filament shape that the Cu filament growth starts at the AE (Cu)/ZnO interface and stops at the CE (Pt or AZO) surface. The overall filament formation process (i.e., Electroforming process) is schematically illustrated in Figs. 3(b)–3(d). The subsequent schematic RESET and SET processes are presented in Figs. 3(e) and 3(f), and 3(g), respectively. For the RESET process with a negative bias voltage applied to the AE (Cu), the filament near the ZnO/CE interface with the highest electrical potential is electrochemically dissolved, switching the device to an OFF-state. The following SET process only needs to rejuvenate the previously ruptured filament segment, resulting in a lower SET voltage compared to the Electroforming process.

Based on the analysis above, we can conclude that the RS mechanism of oxide-based ECM cells is much different from that of sulfide- and selenide-based ones. It has been reported that compared to oxides, sulfides and selenides can allow faster ion transport due to the long-range disorder in these materials.[41,42] For sulfide- and selenide-based ECM cells, Cu ions reach the counter electrode in a very short time under the high electric field, which are reduced on the counter electrode surface. Thus, Cu filaments grow from the counter electrode to the active electrode. However, in the case of oxide-based cells, it will take a longer time for Cu
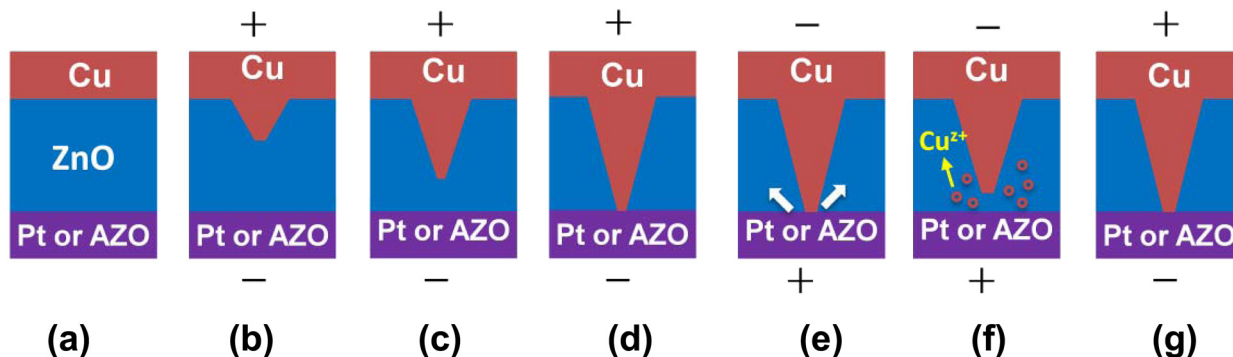
FIG. 3. (Color online) Schematic (a) pristine state, (b)–(d) Electroforming process, (e) and (f) RESET process, and (g) SET process of the Cu/ZnO/Pt (or AZO) ECM cells. Note that the voltage for Electroforming should be higher than that for SET.

ions to transport from the active electrode to the counter electrode since oxides have a Cu ion diffusion coefficient smaller than that of sulfides and selenides. Cu ions are apt to be reduced before they reach the counter electrode resulting in a filament growth direction from the active electrode to the counter electrode.

In summary, we have investigated the asymmetric *I–V* characteristics in the OFF-state of Cu/ZnO/Pt and Cu/ZnO/AZO ECM cells. The results indicate that the Cu filament rupture and rejuvenation occur at the cathodic interface, i.e., ZnO/Pt (or AZO) interface. Considering that the filament is always ruptured at the weakest position, the metal filament should have a conical shape, where wider and narrower diameters are formed at the anodic (Cu) and cathodic (Pt or AZO) interfaces, respectively. It is inferred that the filament growth starts at the Cu electrode surface and stops at the Pt or AZO surface.

[1]R. Waser and M. Aono, Nature Mater. **6**, 833 (2007).
[2]I. Valov, R. Waser, J. R. Jameson, and M. N. Kozicki, Nanotechnology **22**, 254003 (2011).
[3]R. Waser, R. Dittmann, G. Staikov, and K. Szot, Adv. Mater. **21**, 2632 (2009).
[4]R. Symanczyk, R. Bruchhaus, R. Dittrich, and M. Kund, IEEE Electron Device Lett. **30**, 876 (2009).
[5]C. Gopalan, Y. Ma, T. Gallo, J. Wang, E. Runnion, J. Saenz, F. Koushan, P. Blanchard, and S. Hollmer, Solid State Electron. **58**, 54 (2011).
[6]D. Kamalanathan, U. Russo, D. Ielmini, and M. N. Kozicki, IEEE Electron Device Lett. **30**, 553 (2009).
[7]R. Bruchhaus, M. Honal, R. Symanczyk, and M. Kund, J. Electrochem. Soc. **156**, H729 (2009).
[8]M. Kund, G. Beitel, C. U. Pinnow, T. Roehr, J. Schumann, R. Symanczyk, K. D. Ufert, and G. Mueller, Tech. Dig. - Int. Electron Devices Meet. **2005**, 754.
[9]N. E. Gilbert and M. N. Kozicki, IEEE J. Solid-State Circuits **42**, 1383 (2007).
[10]L. Chen, Z. G. Liu, Y. D. Xia, K. B. Yin, L. G. Gao, and J. Yin, Appl. Phys. Lett. **94**, 162112 (2009).
[11]Z. Wang, P. B. Griffin, J. McVittie, S. Wong, P. C. McIntyre, and Y. Nishi, IEEE Electron Device Lett. **28**, 14 (2007).
[12]P. van der Sluis, Appl. Phys. Lett. **82**, 4089 (2003).
[13]H. X. Guo, L. G. Gao, Y. D. Xia, K. Jiang, B. Xu, Z. G. Liu, and J. Yin, Appl. Phys. Lett. **94**, 153504 (2009).
[14]Y. C. Yang, F. Pan, Q. Liu, M. Liu, and F. Zeng, Nano Lett. **9**, 1636 (2009).
[15]F. Zhuge, S. S. Peng, C. L. He, X. J. Zhu, X. X. Chen, Y. W. Liu, and R. W. Li, Nanotechnology **22**, 275204 (2011).
[16]L. Shi, D. S. Shang, J. R. Sun, and B. G. Shen, Phys. Status Solidi (RRL) **4**, 344 (2010).
[17]Y. C. Yang, F. Pan, and F. Zeng, New J. Phys. **12**, 023008 (2010).
[18]M. N. Kozicki, C. Gopalan, M. Balakrishnan, and M. Mitkova, IEEE Trans. Nanotechnol. **5**, 535 (2006).
[19]C. Schindler, G. Staikov, and R. Waser, Appl. Phys. Lett. **94**, 072109 (2009).
[20]S. C. Puthentheradam, D. K. Schroder, and M. N. Kozicki, Appl. Phys. A **102**, 817 (2011).
[21]T. Sakamoto, N. Banno, N. Iguchi, H. Kawaura, H. Sunamura, S. Fujieda, K. Terabe, T. Hasegawa, and M. Aono, Dig. Tech. Pap. - Symp. VLSI Technol. **2007**, 38.
[22]K. Tsunoda, Y. Fukuzumi, J. R. Jameson, Z. Wang, P. B. Griffin, and Y. Nishi, Appl. Phys. Lett. **90**, 113501 (2007).
[23]Q. Liu, C. M. Dou, Y. Wang, S. B. Long, W. Wang, M. Liu, M. H. Zhang, and J. N. Chen, Appl. Phys. Lett. **95**, 023501 (2009).
[24]T. Kever, U. Bottger, C. Schindler, and R. Waser, Appl. Phys. Lett. **91**, 083506 (2007).
[25]S. H. Jo and W. Lu, Nano Lett. **8**, 392 (2008).
[26]F. Zhuge, W. Dai, C. L. He, A. Y. Wang, Y. W. Liu, M. Li, Y. H. Wu, P. Cui, and R. W. Li, Appl. Phys. Lett. **96**, 163505 (2010).
[27]K. M. Kim, D. S. Jeong, and C. S. Hwang, Nanotechnology **22**, 254002 (2011).
[28]Y. Hirose and H. Hirose, J. Appl. Phys. **47**, 2767 (1976).
[29]M. N. Kozicki and M. Mitkova, J. Non-Cryst. Solids **352**, 567 (2006).
[30]T. Fujii, M. Arita, Y. Takahashi, and I. Fujiwara, Appl. Phys. Lett. **98**, 212104 (2011).
[31]D. H. Kwon, K. M. Kim, J. H. Jang, J. M. Jeon, M. H. Lee, G. H. Kim, X. S. Li, G. S. Park, B. Lee, S. Han *et al*., Nat. Nanotechnol. **5**, 148 (2010).
[32]X. Wu, K. Li, N. Raghavan, M. Bosman, Q. X. Wang, D. Cha, X. X. Zhang, and K. L. Pey, Appl. Phys. Lett. **99**, 093502 (2011).
[33]J. G. Lu, Z. Z. Ye, F. Zhuge, Y. J. Zeng, B. H. Zhao, and L. P. Zhu, Appl. Phys. Lett. **85**, 3134 (2004).
[34]F. Zhuge, L. P. Zhu, Z. Z. Ye, D. W. Ma, J. G. Lu, J. Y. Huang, F. Z. Wang, Z. G. Ji, and S. B. Zhang, Appl. Phys. Lett. **87**, 092103 (2005).
[35]F. Zhuge, L. P. Zhu, Z. Z. Ye, J. G. Lu, H. P. He, and B. H. Zhao, Chem. Phys. Lett. **437**, 203 (2007).
[36]L. J. Brillson and Y. C. Lu, J. Appl. Phys. **109**, 121301 (2011).
[37]X. S. Wu, M. Sprinkle, X. B. Li, F. Ming, C. Berger, and W. A. de Heer, Phys. Rev. Lett. **101**, 026801 (2008).
[38]S. H. Jee, N. Kakati, S. H. Lee, H. H. Yoon, and Y. S. Yoon, Appl. Phys. Lett. **98**, 142108 (2011).
[39]K. B. Sundaram and A. Khan, J. Vac. Sci. Technol. A **15**, 428 (1997).
[40]W. Wang, Q. Feng, K. Jiang, J. Huang, X. Zhang, W. Song, and R. Tan, Appl. Surf. Sci. **257**, 3884 (2011).
[41]J. Q. Huang, L. P. Shi, E. G. Yeo, K. J. Yi, and R. Zhao, IEEE Electron Device Lett. **33**, 98 (2011).
[42]N. Banno, T. Sakamoto, N. Iguchi, H. Sunamura, K. Terabe, T. Hasegawa, and M. Aono, IEEE Trans. Electron Devices **55**, 3283 (2008).